Reptation in linear systems

G. Sartoni and J. M. J. van Leeuwen
Instituut Lorentz, Rijks Universiteit Leiden, 2300 RA Leiden, The Netherlands
(Received 14 August 1997)

A model suitable for reptation in linear systems under a driving field is proposed. Its dynamics is based on the decoupling of opposite repton jumps, and is essentially different from reptation in higher dimensions, namely the Rubinstein-Duke model (RDM). The stationary density and correlation functions are calculated perturbatively in the driving field. A meaningful mean field theory is also derived. Diffusion exhibits a strong drift velocity and band collapse. Also a peculiar scaling behavior is found. The results address the sensitivity of reptation process to the rules of motion and the boundary conditions. [S1063-651X(97)12912-9]

PACS number(s): 83.20.Fk, 05.40.+j, 82.45.+z

I. INTRODUCTION

The process of reptation is generally regarded as one of the basic mechanisms governing polymer diffusion through a gel matrix. Its main ingredient is the accumulation of polymer units inside a gel pore, and the subsequent redistribution to neighboring pores. After the introduction of the idea by de Gennes [1], it has developed into a basic ingredient in the understanding of the polymer dynamics in a gel. Recently, Rubinstein [2] and Duke [3] have given a lattice realization of the reptative motion, which makes it possible to simulate reptation and to test the basic features in a quantitative way. In the Rubinstein-Duke model (RDM) gel pores are represented as a regular lattice of cells separated from one another by site obstacles. The polymer is schematized as a chain whose basic units, *the reptons*, are segments of the order of its persistence length. This way reptons can move without mutual tension along the channel (or tube) of cells that the polymer traces out. Polymer self-avoidance is neglected and chain continuity is implemented by the requirement that neighboring reptons occupy either the same or adjacent pores. Diffusion is realized by subsequent jumps of reptons to neighboring cells along the tube, whereas end reptons may also move to outer pores, feeding thus new cells to the tube.

If a reference direction is chosen along the lattice diagonal, the relative coordinate between successive reptons may assume only three values: $\{-1,0,1\}$; see Fig. 1. Likewise, a repton may move either up or down with respect to the reference direction. Thus reptation can be depicted as a one-dimensional diffusion process with ± 1 or 0 states and upward or downward moves. Acidic polymers, like DNA, become charged when solved in a gel. If an electric field is applied to the solution, the diffusion is driven along the field, which is chosen along the reference direction. This feature is incorporated into the RDM by assigning a bias to hopping rates, according to field direction and strength.

Despite its schematic nature the RDM exhibits a very rich and complex behavior and both theoretical results [2,4,5,8] and simulations [3,6,7] compare quite well with experiments on polymer diffusion in gels [9]. The main physical achievement of the RDM consist of grasping the essential features of chain reptation, which induces strong correlation among segments. The process of tube renewal at either ends of the polymer is also very well accomplished in the model. Presence of strong intersegment correlation represents, however, the main source of failure of many attempts towards a theoretical solution of the model, which is particularly resistant, e.g., to any perturbative approach, notwithstanding the several steps forward that have been made [2,4,5,8].

Although the rules of motion in the Rubinstein-Duke model (RDM), to be given below, are simple and natural, the analysis of the model is complicated and has so far eluded a comprehensive understanding. The model contains two parameters: the length N and the driving field E. The limit $E \to 0$ for fixed (large) N is well understood. It leads amongst

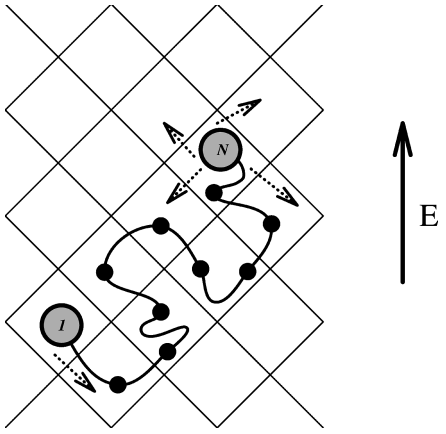

FIG. 1. Repton model of polymer diffusion through a gel. Gel pores are represented as a regular d-dimensional lattice of cells (here $d=2$). Lattice sites represents obstacles to the motion of polymer which thus sneaks from cell to cell. Polymer is conceived as a chain of $N+1$ reptons, which represent its persistence length units. $\vec{E}$ is the driving field serving also as a reference direction. Being x_j the coordinate along $\vec{E}$ of jth repton, then relative displacement of two neighboring reptons, $y_j = x_j - x_{j-1}$, may assume three values: $y_j = +1,0,-1$ in lattice units. Reptons may hop either up, at a rate $B = \exp\varepsilon/2$, or down, at a rate B^{-1}. Each move corresponds to exchange the state of two neighboring y_j, one of which is 0, and the other $+1$ or -1. So that chain motion projected along $\vec{E}$ may be regarded as a 1d diffusion process of $+1$ and -1 particles along N sites with open boundary conditions, because end reptons may hop to unoccupied cells, thus providing other $+1$'s or -1's. The state vector is $\underline{y} = (y_1, \ldots, y_N)$. Considering the example here displayed, $N=10$ and $\underline{y} = (-1,+1,0,+1,+1,-1,0,+1,+1,0)$.

 © 1998 The American Physical Society

others to a drift velocity $\mathcal{V}$ which is proportional to E and inversely proportional to N. Less understood is the scaling limit in which $E\to 0$ and $N\to\infty$ with an appropriate combination of powers of E and N kept fixed. This scaling limit may be regarded as the thermodynamic limit for the stationary state. In contrast to equilibrium one cannot simply study the limit $N\to\infty$ at fixed (small) E, as this leads to situations where the stationary state is never reached as the limit of an arbitrary initial state.

This paper is a contribution to the understanding of the sensitivity of the scaling limit with respect to the details of the rules of motion of the RDM. We will exploit the ambiguity, inherent to the RDM, in the mapping from the tube configuration to the one-dimensional (1D) diffusion process representation, to define a simpler repton model which, in 1D, would be more faithful to the spirit of the motion rules as the actual 1D version of the RDM is. As it will appear, the model is not trivial at all; a systematic expansion in the driving field is feasible and features a well defined scaling limit theory. Moreover a mean field approximation provides an explicit scaling solution which compares also quite well with numerical simulations, both qualitatively and quantitatively. The results are quite different from the physics of the RDM, showing that the motion rules of the RDM are well taken in a higher dimensional embedding matrix and shedding light on the intricate correlations which develop in the stationary state of the RDM.

In the following section we introduce the model and the appropriate formalism to deal with the average properties of polymer diffusion, which are then derived in Sec. III from the microscopic model. The perturbative theory of density and correlation functions is developed in Sec. IV, and its continuum, scaling limit is presented in Sec. V. In Sec. VI we work out a mean field formulation of the problem, and in Sec. VII data from Monte Carlo simulations are compared to analytic results. Section VIII is devoted to conclusions. Appendixes A and B illustrate, respectively, a convenient reformulation of the problem in spin language, and the details about the perturbative expansion.

II. REPTON MODEL AND QUANTUM HAMILTONIAN FORMALISM

As mentioned, in the RDM the gel matrix where diffusion takes place is represented by a d-dimensional hypercubic lattice of cells (gel pores), whereas each lattice site is an obstacle to polymer displacement. The polymer is a chain of $N+1$ reptons connected by N segments. The chain moves through the cells according to usual rules for the RDM: (i) reptons may move diagonally from pore to pore; (ii) internal reptons can move only to pores that the chain already occupies, thus ensuring that reptation is the only diffusion mechanism; (iii) in each pore along the chain there must be at least one repton; (iv) end reptons may also move to neighboring empty cells.

To make it also a model for electrophoresis, a small charge q is assigned to each repton and an electric field, E, is applied along the lattice diagonal, fixing also the reference direction. Thus spatial symmetry is broken, and upward-move rates are biased by a factor

$$B=\exp(\varepsilon/2),\quad \varepsilon=\frac{qlE}{k_BT}, \tag{1}$$

while downward moves are biased by a factor B^{-1}. l is the projection of the lattice constant along the reference direction.

Taking x_j as the coordinate of jth repton along the preferred direction (see, e.g., Fig. 1), polymer configuration can be expressed in terms of the N relative coordinates: $y_j=x_j-x_{j-1}$, $j=2,3,\ldots,N+1$, corresponding also to the orientation of the segment connecting two neighboring reptons (see Fig. 1).

The probability density, $P(\boldsymbol{y},\tau)$, for chain configuration $\boldsymbol{y}=(y_1,y_2,\ldots,y_N)$ at time τ, evolves according to the master equation

$$\frac{dP(\boldsymbol{y},\tau)}{d\tau}=\sum_{\boldsymbol{y}'}\left[W(\boldsymbol{y}|\boldsymbol{y}')P(\boldsymbol{y}',\tau)-W(\boldsymbol{y}'|\boldsymbol{y})P(\boldsymbol{y},\tau)\right], \tag{2}$$

where $W(\boldsymbol{y}|\boldsymbol{y}')$ are transition rates, to be specified below.

In view of a more convenient description, the model may be rewritten in a lattice-gas language, exploiting a quantum Hamiltonian formalism. Consider again the chain of $N+1$ reptons, each segment y_j is regarded as a site which may be either empty or occupied by: an A-particle, $y_j=1$, or a B-particle, $y_j=-1$. Particles may hop to neighboring empty sites and be created or annihilated at both ends. The stochastic time evolution of the system is described by a Schrödinger-like equation:

$$\frac{d|P(\tau)\rangle}{d\tau}=\mathcal{H}|P(\tau)\rangle, \tag{3}$$

where

$$|P(\tau)\rangle=\sum_{\boldsymbol{y}}P(\boldsymbol{y},\tau)|\boldsymbol{y}\rangle,\quad \langle\boldsymbol{y}'|\mathcal{H}|\boldsymbol{y}\rangle=W(\boldsymbol{y}'|\boldsymbol{y}). \tag{4}$$

Conservation of probability is equivalent to the relation

$$\langle s|\mathcal{H}=0;\quad \langle s|=\sum_{\boldsymbol{y}}\langle\boldsymbol{y}|. \tag{5}$$

$\langle s|$ is called the projection state and it is used to define time-dependent average of an observable, say $\mathcal{O}(\boldsymbol{y})$, as

$$\langle\mathcal{O}(\tau)\rangle=\langle s|\mathcal{O}(\boldsymbol{y})|P(\tau)\rangle=\langle s|\mathcal{O}(\boldsymbol{y})e^{\mathcal{H}\tau}|P(0)\rangle. \tag{6}$$

The definition of the stochastic operator $\mathcal{H}$, will then determine the repton model completely.

The A particles exclude each other and the same holds for the B particles. Also the A particles exclude the B particles and vice versa. So we have to use hard-core boson operators or rather spin-1 operators. We take $a_j^\dagger=M_j^{12}$, $a_j=M_j^{21}$, $b_j^\dagger=M_j^{32}$, $b_j=M_j^{23}$ as creation and annihilation operators of A particles and B particles, respectively, on site j. $n_j^a=M_j^{11}$ and $n_j^b=M_j^{33}$ are the corresponding site number operators of particles, and $n_j^0=1-n_j^a-n_j^b=M_j^{22}$. M_j^{pq} is a 3×3 matrix with elements $(M_j^{pq})_{\mu,\nu}=\delta_{p,\mu}\delta_{q,\nu}$ acting on site j [10]. The commutation relations follow from the matrix representation of these operators. Thus the stochastic operator is

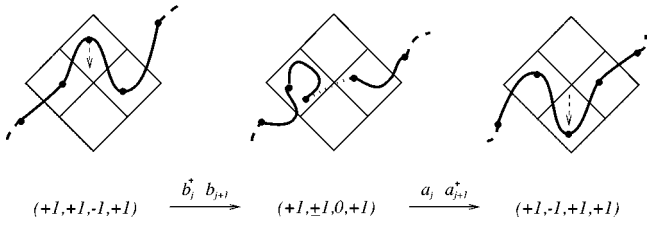

FIG. 2. Example of an unremovable hair-pin configuration. If double occupancy of a $+1$ and -1 would be allowed this might be easily eliminated, e.g., by means of the process sketched here, leading then to unphysical consequences. In the second snapshot dotted line represents the 0 segment virtually going through the obstacle.

$$\mathcal{H}=\beta_1(B)+\beta_N(B^{-1})+\sum_{j=1}^{N-1}\mathcal{T}_j(B), \tag{7}$$

where

$$\beta_j(B)=B(a_j+db_j^\dagger+n_j^b-1)+B^{-1}(da_j^\dagger+b_j+n_j^a-1), \tag{8a}$$

$$\mathcal{T}_j(B)=B(a_j^\dagger a_{j+1}+b_jb_{j+1}^\dagger-n_j^0n_{j+1}^a-n_j^bn_{j+1}^0)+B^{-1}(a_ja_{j+1}^\dagger+b_j^\dagger b_{j+1}-n_j^an_{j+1}^0-n_j^0n_{j+1}^b). \tag{8b}$$

As is noted, the dimensionality d survives only as a parameter in the d-fold degeneracy of moves stretching end-segments in β_1 and β_N. The similarity with quantum mechanics is not as powerful as one would like it to be, since $\mathcal{H}$ is not Hermitian and an *ad hoc* definition of time-dependent average is required; see Eq. (6).

As double site-occupancy is forbidden, the motion rules as described by the interaction terms in $\mathcal{T}_j$ do not allow removal of ''hair-pin'' configurations such as that depicted in Fig. 2. The first and last state, which are different by the order of the intermediate pair $+1,-1$, cannot be transformed into each other by an allowed intermediate step. The one drawn leaves an empty cell in the path of the polymer and disrupts therefore the integrity of the chain. In the subsequent Fig. 3 a sequence of configurations is drawn which is quite well possible in the spirit of the RDM. The first and last configuration are described by the same sequences as in Fig. 2. The intermediate state is formally not allowed by the motion rules of the RDM, but perfectly correct in the spirit of repton-modelization of polymer diffusion. However in RDM the d-dimensional chain is mapped onto a 1D process, which washes out the distinction between the configurations of

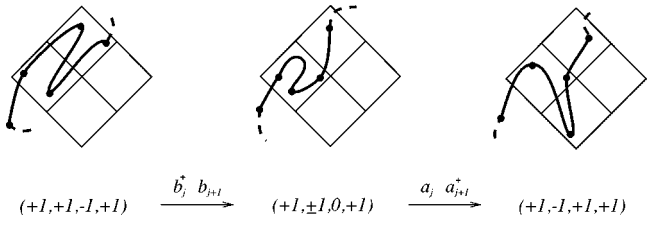

FIG. 3. Example of a removable hair-pin configuration which might be eliminated through a sequence of two moves, displayed here, provided double occupation, ± 1, is allowed to segment states.

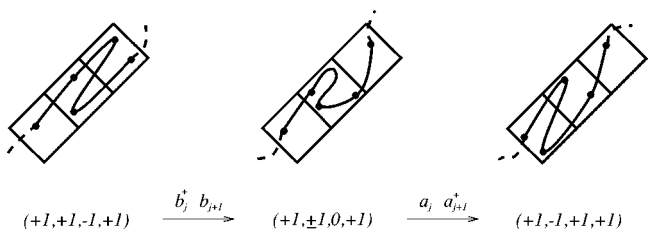

FIG. 4. Here a 1D repton model is shown, where the quick inversion of a folded configuration through a double occupancy dynamics is a realistic process.

Figs. 2 and 3. Therefore a conceptually legitimate process such as in Fig. 3 is then equally forbidden as that in Fig. 2. Since every cell has d upper or lower nearest neighbors, the RDM neglects removable hair-pin configurations, such as in Fig. 3, once every d times. Hence it becomes more and more accurate as d increases. In one dimension, constraints implied by interaction terms in Eq. (7) are thus too strict, there are actually no obstacles to the polymer motion and any loop may be removed (see, e.g., Fig. 4). So we are led to consider a 1D repton model in which the A particles and B particles may interchange via the process sketched in the middle of Fig. 3 or equivalently in the sequence of Fig. 4. By allowing the simultaneous presence of an A and B particle in the same pore, a ± 1 occupation, each segment can be in four possible states: $0,+1,-1,\pm 1$. We take the particle operators $a^\dagger$ and $b^\dagger$ as $a^\dagger=a^\dagger\otimes\mathbf{I}$ and $b^\dagger=\mathbf{I}\otimes b^\dagger$, acting on a product space: $|y_j\rangle=|y_j\rangle_a\otimes|y_j\rangle_b$. This way double occupation is permitted and the annihilation and creation operators fulfill the standard hard-core boson commutation relation (commuting on different segments and anticommuting on the same segment). Thus we are led to the following stochastic operator:

$$\begin{aligned}\mathcal{H}=&\sum_{j=2}^{N}[B(a_{j-1}^\dagger a_j-a_{j-1}a_{j-1}^\dagger a_j^\dagger a_j)+B^{-1}(a_{j-1}a_j^\dagger\\&-a_{j-1}^\dagger a_{j-1}a_ja_j^\dagger)]+B(a_N^\dagger-a_Na_N^\dagger)+B^{-1}(a_N-a_N^\dagger a_N)\\&+B^{-1}(a_1^\dagger-a_1a_1^\dagger)+B(a_1-a_1^\dagger a_1)+\sum_{j=2}^{N}[B^{-1}(b_{j-1}^\dagger b_j\\&-b_{j-1}b_{j-1}^\dagger b_j^\dagger b_j)+B(b_{j-1}b_j^\dagger-b_{j-1}^\dagger b_{j-1}b_jb_j^\dagger)]\\&+B^{-1}(b_N^\dagger-b_Nb_N^\dagger)+B(b_N-b_N^\dagger b_N)+B(b_1^\dagger-b_1b_1^\dagger)\\&+B^{-1}(b_1-b_1^\dagger b_1).\end{aligned} \tag{9}$$

We take this operator as defining our one-dimensional model. The great simplification is the decoupling of the motion of the $+1$'s and -1's. Indeed $\mathcal{H}=\mathcal{H}_a(B)+\mathcal{H}_b(B)$, hence the probability density factorizes: $|P(\tau)\rangle=|P_a(\tau)\rangle\otimes|P_b(\tau)\rangle$. Moreover, since $\mathcal{H}_b(B)=\mathcal{H}_{a=b}(B^{-1})$, $+1$'s and -1's exhibit the same dynamics under opposite field, and one needs to concentrate only on one species of particles. In the remainder we will focus our attention on $+1$ segments only, namely on $a_j^\dagger$ operators, then, unless otherwise specified, an a label appended to any operator or observable will be always understood.

Decoupling upward segments from downward ones does not make the model trivial. For instance the stationary prob-

ability density does not factorize into the product of single segment densities, contrary to what one might expect. Indeed it is easily seen that the state

$$|P_{\text{prod}}\rangle=\prod_{j=1}^{N}(q_j+p_j a_j^\dagger)|0\rangle, \quad q_j+p_j=1, \tag{10}$$

where p_j is the average density of A particle at segment j, is stationary, i.e., $\mathcal{H}|P_{\text{prod}}\rangle=0$, if

$$Bq_{j-1}p_j-B^{-1}p_{j-1}q_j=0 \quad (j=2,\ldots,N-1), \tag{11a}$$

$$Bp_1-B^{-1}q_1=0, \tag{11b}$$

$$Bq_N-B^{-1}p_N=0, \tag{11c}$$

whose only solution is the trivial zero-field one: $p_j=\frac{1}{2}\forall j=1,2,\ldots,N$ and $B=1$. Thus, strictly speaking, in the stationary regime segments are correlated, but as we shall see in the remainder, long chains possess remarkable mean field properties. Since polymer diffusion process is conveniently described in terms of average quantities like drift velocity, $\mathcal{V}$ and curvilinear velocity, $\mathcal{J}$, we are to derive the corresponding time evolution equations from the microscopic dynamics, and eventually obtain an approximated solution.

III. PARTICLE DENSITY AND CURRENT

A particles represent upward segments, the density operator $n_j=a_j^\dagger a_j$ measures the density of $+1$ at segment j. Its evolution equation is obtained from Eqs. (3,6) as

$$\frac{d}{d\tau}\langle n_j\rangle=\langle s|n_j\mathcal{H}|P(\tau)\rangle=\langle s|[n_j,\mathcal{H}]|P(\tau)\rangle \tag{12}$$

since, due to Eq. (5), in general

$$\langle\mathcal{O}(\mathbf{y})\mathcal{H}\rangle=\langle[\mathcal{O}(\mathbf{y}),\mathcal{H}]\rangle. \tag{13}$$

$\langle s|$ possesses another useful property, $\langle s|=\langle 0|\Pi_{j=1}^{N}(1+a_j)$, so

$$\langle s|a_j^\dagger\mathcal{O}(\mathbf{y})|P(\tau)\rangle=\langle(1-n_j)\mathcal{O}(\tau)\rangle;$$

$$\langle s|a_j\mathcal{O}(\mathbf{y})|P(\tau)\rangle=\langle n_j\mathcal{O}(\tau)\rangle, \tag{14}$$

and the commutator average, $\langle[n_j,\mathcal{H}]\rangle$, is easily calculated in terms of n_j only. Simple algebra yields then the continuity equation

$$\frac{d}{d\tau}\langle n_j\rangle=\langle J_{j-1}\rangle-\langle J_j\rangle, \tag{15}$$

where particle currents, $\langle J_j\rangle$, are defined as

$$\langle J_j\rangle=B^{-1}\langle n_j(1-n_{j+1})\rangle-B\langle(1-n_j)n_{j+1}\rangle$$

$$(j=1,2,\ldots,N-1), \tag{16a}$$

$$\langle J_0\rangle=B^{-1}\langle 1-n_1\rangle-B\langle n_1\rangle, \tag{16b}$$

$$\langle J_N\rangle=B^{-1}\langle n_N\rangle-B\langle 1-n_N\rangle. \tag{16c}$$

In the simple case $\varepsilon=0$, everything is homogeneous, $\langle n_j\rangle=\frac{1}{2}$, so it is convenient to shift every density by such zero-field solution. The new density operators are $m_j=n_j-\frac{1}{2}$ and have the average bounded by $-\frac{1}{2}\leqslant\langle m_j\rangle\leqslant\frac{1}{2}$. In zero field $\langle m_j\rangle=0$. So m_j behave as a spin-$\frac{1}{2}$ variable. Furthermore one may use a different field parameter, namely

$$t=\frac{B-B^{-1}}{B+B^{-1}}=\tanh\frac{\varepsilon}{2}, \tag{17a}$$

and then

$$B=\frac{(1+t)}{2}(B+B^{-1}), \quad B^{-1}=\frac{(1-t)}{2}(B+B^{-1}). \tag{17b}$$

Since the system is symmetric under exchange of $+1$'s with 0's and simultaneous field reversion (see Appendix A for a detailed discussion about symmetries of $\mathcal{H}$), one has

$$\langle m_j\rangle(t)=\langle a_j a_j^\dagger-\tfrac{1}{2}\rangle=-\langle m_j\rangle(-t). \tag{18}$$

Hence, $\langle m_j\rangle(t)$ is odd in t. Likewise, the average of any product of an odd (even) number of different m_j's is odd (even) in t. The dynamics is also invariant when $+1$'s and 0's are interchanged and the segment labelling order is reversed, $j\to N+1-j$. This property implies $\langle m_j\rangle$ is symmetric around the middle point of the chain,

$$\langle m_j\rangle=-\langle m_{N+1-j}\rangle \tag{19}$$

and thus $\langle m_{(N+1)/2}\rangle=0$.

The stationary state is obtained imposing $d/d\tau\langle m_j\rangle=0$, which, through Eq. (15), implies

$$\langle J_j\rangle=\mathcal{J}\ \forall j=1,2,\ldots,N, \tag{20}$$

with $\mathcal{J}$ stationary current, constant through the chain. Combining this with definitions (16), one is left with the system

$$J=\langle m_j\rangle-\langle m_{j+1}\rangle+\frac{t}{2}[4\langle m_j m_{j+1}\rangle-1]$$

$$\times(j=1,2,\ldots,N-1), \tag{21a}$$

$$J=-2\langle m_1\rangle-t, \tag{21b}$$

$$J=2\langle m_N\rangle-t, \tag{21c}$$

where $J=(2/B+B^{-1})\mathcal{J}$ is also an odd function of t, like $\mathcal{J}$, since it is a current and $t\sim\mathcal{O}(\varepsilon)$. Equation (21) is typical for an open hierarchy with more unknowns than equations in each stage. If we had knowledge about the average of the product $\langle m_j m_{j+1}\rangle$, the values of the single averages $\langle m_j\rangle$ would be determined. Anticipating that the average of the product is of a higher order we omit it here to get a notion of the structure of the lowest order approximation of m_j. The equations are easily solved and the solution is denoted as

$$\langle m_j\rangle=tm_j^{(1)}+\mathcal{O}(t^3), \quad j=tj^{(1)}+\mathcal{O}(t^3), \tag{22}$$

with

$$m_j^{(1)}=\frac{2j-N-1}{4N} \quad (j=1,2,\ldots,N), \tag{23a}$$

$$J^{(1)}=-\frac{N+1}{2N}. \tag{23b}$$

By omitting the product of the averages the solution (23) becomes strictly proportional to t. Note that this solution obeys the symmetry relations (18) and (19).

IV. PERTURBATIVE EXPANSION OF DENSITY, CURRENT, AND CORRELATION FUNCTION

When ε is small, so is $t=\frac{\varepsilon}{2}+O(\varepsilon^3)$, providing an ideal weak field expansion parameter. We make the following ansatz for the expansions in powers of t:

$$J=tJ^{(1)}+t^3J^{(3)}+O(t^5), \tag{24a}$$

$$\langle m_j\rangle=tm_j^{(1)}+t^3m_j^{(3)}+O(t^5), \tag{24b}$$

$$\langle m_jm_l\rangle=t^2m_{j,l}^{(2)}+t^4m_{j,l}^{(4)}+O(t^6), \tag{24c}$$

$$\langle m_jm_km_l\rangle=t^3m_{j,k,l}^{(3)}+O(t^5). \tag{24d}$$

The powers that are included are compatible with the symmetry relation (18). The essential point of the proposed expansion is that the average of a product of n variables m_j starts with the power t^n. For the product of a pair this is self-evident, since a zeroth order is excluded, due to the lack of correlations in the undriven system. This justifies the solution (23) as the first order in t. The justification for the ansatz (24) is based on the fact that for every product of allowed combination (no equal indices) one can write the equation of motion as

$$\begin{aligned}\frac{d}{d\tau}\langle m_jm_l\cdots m_k\rangle&=\langle[m_jm_l\cdots m_k,\mathcal{H}]\rangle\\&=\langle m_jm_l\cdots[m_k,\mathcal{H}]\rangle+\cdots\\&\quad+\langle[m_j,\mathcal{H}]m_l\cdots m_k\rangle.\end{aligned} \tag{25}$$

The stationarity condition requires the left-hand side to be zero. Now the commutator $[m_j,\mathcal{H}]$ involves terms linear in the m_j and coupling terms containing the product of the latter and its neighbors, $m_{j\pm1}$. Thus a product of n factors couples through the Hamiltonian to a product of $n+1$ factors, as we already encountered in Eq. (21) for $n=1$. By the ansatz that term starts out with an $O(t^{n+1})$ and the coupling in $\mathcal{H}$ involves another factor t. So the lowest order of the product of n factors can be calculated without information of the higher correlation functions. Furthermore higher orders of the expansion of the n-product average, say $O(t^{n+2p})$, are coupled to $O(t^{n+1+2(p-1)})$ of the $(n+1)$ product, which have been calculated at a previous stage of the expansion. So, as we know $m_j^{(1)}$ we can recursively build up the solution in any order. To illustrate the method we first write down the equation for $m_j^{(1)}$, which is obtained expanding Eqs. (21) in t:

$$J^{(1)}=m_j^{(1)}-m_{j+1}^{(1)}-\frac{1}{2}, \tag{26a}$$

$$J^{(1)}=2m_N^{(1)}-1, \tag{26b}$$

$$J^{(1)}=-2m_1^{(1)}-1, \tag{26c}$$

with the solution anticipated in Eq. (23). Then we may proceed further to consider $m_{j,l}^{(2)}$. The general term is easy (see Appendix B):

$$4m_{j,l}^{(2)}=m_{j-1,l}^{(2)}+m_{j,l+1}^{(2)}+m_{j+1,l}^{(2)}+m_{j,l-1}^{(2)} \quad (2\leqslant j\leqslant l-2;l\leqslant N-1). \tag{27}$$

Special equations hold for the cases where $j=1$, $j=l-1$ and $l=N$, which connect them to the lower order $m_j^{(1)}$. We have spelled them out in Appendix B. The form of Eq. (27) is that of the discrete Laplace equation. The solution is determined in Appendix B and reads

$$m_{j,l}^{(2)}=\frac{2N}{N-1}m_j^{(1)}m_l^{(1)}-\frac{N+1}{4(N-1)}(m_j^{(1)}-m_l^{(1)})-\frac{N+1}{16(N-1)}. \tag{28}$$

The correlation is long-ranged because the actual form of $m_{j,l}^{(2)}$ is essentially determined by boundary conditions (BC) that globally influence the solution. Concerning in particular adjacent segments, $l=j+1$, we have

$$m_{j,j+1}^{(2)}=\frac{2N}{N-1}(m_j^{(1)})^2+\frac{m_j^{(1)}}{(N-1)}-\frac{(N+1)(N-2)}{16N(N-1)}. \tag{29}$$

This is a convex parabola, hence adjacent segments have a stronger tendency to be anticorrelated in the bulk of the chain.

Knowing $m_{j,l}^{(2)}$, $m_j^{(3)}$ can be calculated. From Eq. (21) the general equation set for $m_j^{(n)}$ $(n>1)$ is

$$J^{(n)}=m_j^{(n)}-m_{j+1}^{(n)}+2m_{j,j+1}^{(n-1)} \ (j=1,2,\ldots,N-1), \tag{30a}$$

$$J^{(n)}=2m_N^{(n)}=-2m_1^{(n)}. \tag{30b}$$

In view of Eq. (19) every observable containing m_j is more conveniently expressed in terms of $m_j^{(1)}$, in place of j, as it directly embodies the symmetry. Given the form of $m_{j,l}^{(2)}$ we may then solve Eq. (30) for $m_j^{(3)}$ by the ansatz $m_j^{(3)}=\kappa_1(m_j^{(1)})^3+\kappa_2m_j^{(1)}$, which provides

$$m_j^{(3)}=\frac{8N^2}{3(N-1)}(m_j^{(1)})^3-\frac{(2N^2-3N+3)}{12(N-1)}m_j^{(1)}, \tag{31a}$$

$$J^{(3)}=-\frac{N+1}{24N}. \tag{31b}$$

We have also calculated the leading order of $\langle m_jm_km_l\rangle$, $m_{j,k,l}^{(3)}$ in terms of $m_j^{(1)}$ and $m_{j,k}^{(2)}$ (see Appendix B for details). This function displays similar global correlation effects determined by BC. We can then proceed further to obtain $m_{j,l}^{(4)}$,

which is a polynomial of fourth order in $m_j^{(1)}$. Then from Eq. (30) we argue that $m_j^{(5)}$ must be of the form

$$m_j^{(5)} = \eta_1 (m_j^{(1)})^5 + \eta_2 (m_j^{(1)})^3 + \eta_3 m_j^{(1)}. \tag{32}$$

Direct substitution yields

$$\eta_1 = \frac{64N^4}{5(N-1)(N-2)}; \quad \eta_2 = \frac{-16N^4+52N^3-4N^2}{9(N-1)(N-2)}, \tag{33}$$

$$\eta_3 = \frac{22N^5-130N^4+235N^3+225N^2-270N-180}{360N(N-1)(N-2)}, \tag{34}$$

and

$$J^{(5)} = \frac{8N^4+33N^3+303N^2-262N-180}{720N^2(N-2)}. \tag{35}$$

Further steps in the perturbative expansion would require knowledge of $\langle m_j m_k m_l m_p \rangle$ and so on.

In the limit $N \to \infty$, the lattice model is amenable of a continuum approximation in terms of $x \sim j/N$, where x derivatives substitute finite differences, neglecting systematically higher orders in $1/N$. In this ''hydrodynamic'' limit $\langle m_x \rangle$, $\langle m_x m_y \rangle$ and so on, are determined by simple (partial) differential equations which we give in the next section.

V. CONTINUUM LIMIT THEORY

When the chain is very long one may neglect the details relating to each single segment at length scales smaller than $1/N$. In a coarse grained description any observable may be considered as a smooth function of the central variable x defined as

$$x = \frac{j-(N+1)/2}{N}. \tag{36}$$

So the continuum analog of Eq. (24) is

$$\langle m_x \rangle = t m^{(1)}(x) + t^3 m^{(3)}(x) + \cdots, \tag{37a}$$

$$\langle m_x m_y \rangle = t^2 m^{(2)}(x,y) + t^4 m^{(4)}(x,y) + \cdots, \tag{37b}$$

$$\langle m_x m_y m_z \rangle = t^3 m^{(3)}(x,y,z) + \cdots. \tag{37c}$$

Considering leading terms in the limit $N \to \infty$ the perturbative results we obtain in Sec. IV and in Appendix B are summarized as

$$J = -\frac{t}{2} - \frac{t}{2N} - \frac{t^3}{24} + \frac{t^5 N}{90} + O(t^7), \tag{38a}$$

$$\langle m_x \rangle = t\left[\frac{x}{2} + t^2 N\left(\frac{x^3}{3} - \frac{x}{12}\right) + t^4 N^2\left(\frac{2}{5}x^5 - \frac{2}{9}x^3 + \frac{11}{360}x\right)\right] + O(t^7) \quad (x \in [-\tfrac{1}{2}, \tfrac{1}{2}]), \tag{38b}$$

$$\langle m_x m_y \rangle = t^2\left\{\frac{xy}{2} - \frac{(x-y)}{8} - \frac{1}{16} + t^2 N\left[\frac{(x^3y+xy^3)}{2} - \frac{(x^3-y^3)}{6} + \frac{(x^2y-xy^2)}{4} - \frac{(x^2+y^2)}{8} - \frac{xy}{12} + \frac{(x-y)}{48} + \frac{1}{48}\right]\right\} + O(t^6) \times (-\tfrac{1}{2} \leqslant x < y \leqslant \tfrac{1}{2}), \tag{38c}$$

$$\langle m_x m_y m_z \rangle = t^3\left[\frac{3}{4}xyz - \frac{(x-z)y}{4} - \frac{(x+z)}{32} - \frac{3}{32}y\right] + O(t^5) \quad (-\tfrac{1}{2} \leqslant x < y < z \leqslant \tfrac{1}{2}). \tag{38d}$$

So we have evidence that in the limit $N \gg 1$, $t^2 N$ has to be the suitable power combination for the thermodynamic scaling limit: $N \to \infty$, $t \to 0$, with $\lambda = t^2 N$ finite. We can implement the scaling limit by the ansatz

$$\langle m_{x_1} \cdots m_{x_n} \rangle = t^n \tilde{m}(x_1, \ldots, x_n; \lambda). \tag{39}$$

In terms of these continuous functions Eq. (21) becomes

$$J = t[\tilde{m}(x;\lambda) - \tilde{m}(x + 1/N;\lambda)] + 2t[t^2 \tilde{m}(x, x + 1/N;\lambda) - \tfrac{1}{4}], \tag{40a}$$

$$J = -2t\tilde{m}(-\tfrac{1}{2} + 1/2N;\lambda) - t = 2t\tilde{m}(\tfrac{1}{2} - 1/2N;\lambda) - t. \tag{40b}$$

In view of the perturbative results we take as scaling form for the J

$$J = t\left(-\frac{1}{2} + \frac{1}{N}\tilde{J}(\lambda)\right). \tag{41}$$

We expand around x and count an order N^{-1} as equivalent to t^2. We then find to leading order

$$\tilde{J}(\lambda) = -\frac{d\tilde{m}(x;\lambda)}{dx} + 2\lambda \tilde{m}(x,x;\lambda) \tag{42}$$

and the boundary conditions

$$\tilde{m}(\tfrac{1}{2};\lambda) = -\tilde{m}(-\tfrac{1}{2};\lambda) = \tfrac{1}{4}. \tag{43}$$

The value of $\tilde{J}(\lambda)$ has to be chosen such that the boundary conditions are fulfilled.

In a similar way we obtain for $\tilde{m}(x,y;\lambda)$ the equation

$$\nabla^2 \tilde{m}(x,y;\lambda) = 2\lambda[\tilde{m}_1(x,x,y;\lambda) + \tilde{m}_2(x,x,y;\lambda) + \tilde{m}_2(x,y,y;\lambda) + \tilde{m}_3(x,y,y;\lambda)] \tag{44}$$

with the boundary conditions

$$\tilde{m}(x, \tfrac{1}{2};\lambda) = \frac{\tilde{m}(x;\lambda)}{4}, \tag{45a}$$

$$\widetilde{m}_1(x,x;\lambda)-\widetilde{m}_2(x,x;\lambda)=\frac{1}{2}\frac{\partial\widetilde{m}(x;\lambda)}{\partial x}, \tag{45b}$$

where

$$\widetilde{m}_k(x_1,\cdots,x_n;\lambda)=\frac{\partial\widetilde{m}(x_1,\cdots,x_n;\lambda)}{\partial x_k}. \tag{46}$$

The general structure of the hierarchy is clear. In the bulk $\widetilde{m}(x_1,\cdots,x_n;\lambda)$ couples to a higher member $\widetilde{m}(x_1,\cdots,x_{n+1},\lambda)$ and at the boundaries to a lower member $\widetilde{m}(x_1,\cdots,x_{n-1};\lambda)$.

Such a hierarchy is difficult to solve. We must either make an assumption of the higher correlation function in terms of the lower ones (as we do in the next section), or make a perturbation expansion in powers of λ (as we have done in the previous section). Due to the fact that the coupling term to the higher correlation function has a factor λ in front, the lower correlation functions decouple in the expansion from the higher ones. As one observes from the result (38) this expansion has the simplifying feature that the terms in the expansion are polynomials in the x_j. So solution of the hierarchy means in essence matching of the coefficients of the polynomials. As we have noticed in Appendix B, one has in general more equations to satisfy than coefficients to play with. However, the equations turn out to have the right interdependency to allow a unique solution.

VI. MEAN FIELD THEORY

Our mean field (MF) ansatz consist of approximating $\widetilde{m}(x,x;\lambda)$ by $[\widetilde{m}(x;\lambda)]^2$ in Eq. (42). This amounts to the usual approximation of the average of a product by the product of the averages. We are thus led to the MF equation

$$\frac{d\widetilde{m}_{\rm MF}(x;\lambda)}{dx}=2\lambda\widetilde{m}^2_{\rm MF}(x,\lambda)-\widetilde{J}_{\rm MF}(\lambda), \tag{47}$$

and the same boundary conditions (43). Equation (47) is straightforwardly integrated, giving

$$m_{\rm MF}(x;\lambda)=tq(\lambda)\tan(2\lambda q(\lambda)x), \tag{48a}$$

$$\widetilde{J}=-2\lambda q^2(\lambda), \tag{48b}$$

with $q(\lambda)$ determined by

$$2q(\lambda)\tan(\lambda q(\lambda))=\tfrac{1}{2}. \tag{49}$$

In limiting cases $q(\lambda)$ is easily calculated

$$q(\lambda)\simeq\frac{1}{2\sqrt{\lambda}}\quad\text{for } q\lambda\ll 1, \tag{50a}$$

$$q(\lambda)\simeq\frac{\pi}{2\lambda}\quad\text{for } \lambda\gg 1. \tag{50b}$$

The solution (48) has the required scaling form and its simplicity allows us to illustrate the main features of reptation process. For $\lambda q\ll 1$, $m_{\rm MF}(x)$ is linear in x as a consequence of slow diffusion of $+1$ segments from the head of the chain, $x=\frac{1}{2}$, where they are supplied at rate B, towards the tail, $x=-\frac{1}{2}$, where they disappear at the same rate. As λ, i.e., t and/or N, increases, the profile of $m(x)$ becomes more and more flat and it squeezes onto the x axis, just to rise or fall down sharply upon approaching respectively $x=1/2$ or $x=-\frac{1}{2}$. In these conditions $+1$ segments are constantly fed to the chain at its head, where they stay to wait a zero segment coming from the bulk. Of course a symmetric scenario applies to zeros created at the chain tail. In the bulk the environment is essentially random, $\langle n_j\rangle=\langle 1-n_j\rangle=\frac{1}{2}$, due to the the mixing of the two opposing streams of $+1$'s and 0's.

We may also compare MF and exact results on the profile, $m(x)$, up to $O(t^5)$. From Eqs. (48) and (49),

$$m_{\rm MF}(x)=t\left[\frac{x}{2}+t^2N\left(\frac{x^3}{6}-\frac{x}{24}\right)+t^4N^2\left(\frac{x^5}{15}-\frac{x^3}{36}+\frac{x}{360}\right)\right]+O(t^7), \tag{51a}$$

$$J_{\rm MF}=-\frac{t}{2}-\frac{t}{2N}+\frac{t^3}{24}-\frac{t^5N}{360}+O(t^7). \tag{51b}$$

When compared with Eq. (38) the discrepancy is of order t^2N, so the MF approximation is expected to fail for $t^2N\sim 1$. The second term in the expansion of $m(x)$ is underestimated by a factor of 2 and the difference increases at higher orders, and indeed $m_{\rm MF}(x)$ remains below $m(x)$ for increasing values of t; compare also Fig. 7. Nevertheless, within this range it provides in a simple form a meaningful determination of chain profile and current. To estimate the degree of accuracy of mean field solution (48) as well as its reliability, a comparison with numerical simulation is also desirable.

Before going on to discuss simulations, it is, however, worth stressing that perturbative results for J are very robust. Indeed in the limit $N\to\infty$ with $\lambda=$const., the corrections are small, of order t^3 or t/N, as shown by Eqs. (51) and (38). Moreover, the discrepancy between the MF and exact value of J becomes irrelevant under such condition. Hence $J=-(t/2)+O(t^3)$ and band collapse is predicted for this repton model in the limit $N\gg 1$. Since J is essentially the drift velocity, $\mathcal{V}=-2J$, so $\mathcal{V}$ is insensitive to N when the latter is large.

VII. COMPARISON WITH THE SIMULATIONS

Monte Carlo (MC) simulations of our repton model have been performed, always restricting to $+1$'s dynamics, with move rules and rates as dictated by $\mathcal{H}_a$. Chains of $N=100$ and 200 segments have been considered. For each value of $t\in]0,1[$, about $2\times N^4$ MC steps have been iterated and, after waiting about N^4 steps for thermalization, chain configurations have been sampled every N steps (i.e., every whole chain sweep) to determine the average densities: $\overline{m_j}=\overline{n_j}-\frac{1}{2}$.

By means of a one-parameter nonlinear fit $q(\lambda)$ is then calculated from $\overline{m_j}$ assuming the MF form

$$\frac{\overline{m(x)}}{t}=q\,\tan(2\lambda qx) \tag{52}$$

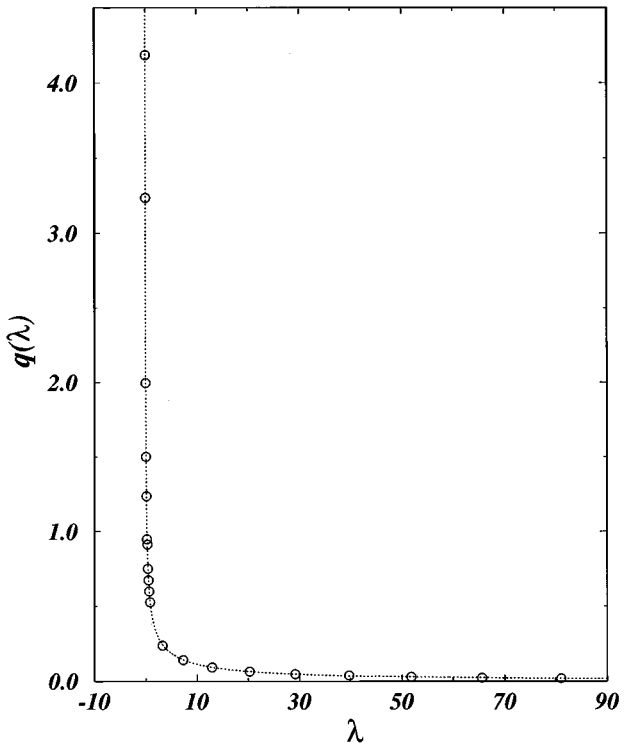

FIG. 5. Plot of parameter $q(\lambda)$ determined by fitting simulation data for segment density, $\overline{m(x)}$, to the expected MF behavior, for $N=100$. Behavior of fitted values (open circles) is in excellent agreement with numerical solution (dashed line) of the equation determining $q(\lambda)$ in the MF theory.

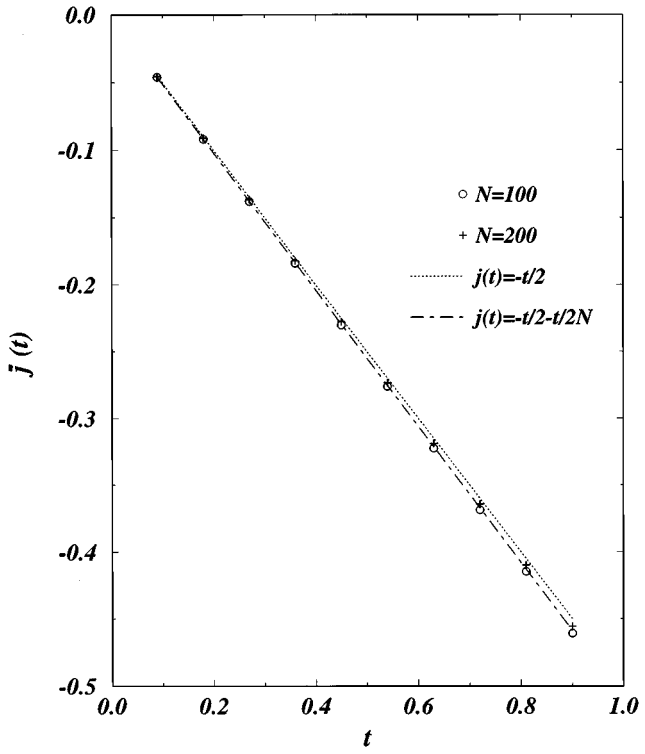

FIG. 6. Average current, $\overline{J(t)}$, of $+1$ segments calculated from simulation of chains of $N=100$ and $N=200$ segments. The asymptotic, $N\to\infty$, prediction, $J=-t/2$, is also plotted for comparison (dotted line). Since N is not very large, $\overline{J(t)}$ departs slightly from the ideal curve due to small t/N corrections (dot-dashed line, with $N=100$), as predicted by perturbative results, Eq. (23).

according to Eq. (48). Fitted values of $q(\lambda)$ are plotted in Fig. 5 against λ. The numerical solution of Eq. (49) is also shown for comparison. Agreement between MF theory and simulation data is excellent.

The average current

$$\overline{J}=\frac{2}{B+B^{-1}}\overline{\mathcal{J}} \tag{53}$$

is also computed and compared with our analytical result: $J\cong -t/2$, in Fig. 6. We obtain a good agreement even though $N\sim 100$, hence for relatively short chains.

Finally Fig. 7 displays the rescaled plot of $\overline{m_j}$ against the MF expectation

$$\frac{m_{\mathrm{MF}}(\chi)}{tq}=\tan(\chi), \tag{54}$$

with $\chi=2\lambda qx$, exploiting the fitted values of $q(\lambda)$. Curves collapse well for smaller t values, while they slightly depart from theoretic prediction when t increases. However, even in the region $\lambda>1$, where MF is expected to fail, the qualitative behavior of $\overline{m_j}$ is well reproduced by such approximation.

Simulations thus provide evidence that the MF theory represents a rather accurate approximation when $\lambda\lesssim 1$, and it is meaningful also for larger values, namely under strong electric field, where correlations are expected to be most relevant.

VIII. DISCUSSION AND CONCLUSIONS

We have considered a genuine one-dimensional version of the Rubinstein-Duke model (RDM) for reptation. In the RDM the configurations of the polymer are mapped on a one-dimensional sequence. In this map the distinction between removable and nonremovable hairpins is washed out (see Figs. 2–4). The higher the dimension of the embedding matrix, the less frequent these removable hairpins occur. In a linear system the paths of the polymer contain only removable hairpins, which makes the dynamics essentially different from the higher dimensional cases. It means that forward $(+1)$ and backward (-1) segments may interchange and when they are allowed to coexist the motion of the two species is completely decoupled. While the RDM may be seen as a spin-1 chain, the linear version maps on a set of two decoupled spin-$\frac{1}{2}$ systems.

The resulting dynamics is still far from trivial due the basic feature of all reptation models that the chain configurations can only be refreshed by shrinking and growing at the ends of the chain. As the linear systems have no internal obstacles the motion of the chain under the influence of a driving field is much faster. Indeed due to decoupled dynamics hairpins are just trailing or removed, e.g., such as those sketched in Fig. 4, essentially at the same rate as a simple repton drift, namely $B-B^{-1}\sim t$. This makes the drift velocity linear in the driving field and *independent* of the chain length N. In the language of electrophoresis it means a total band collapse.

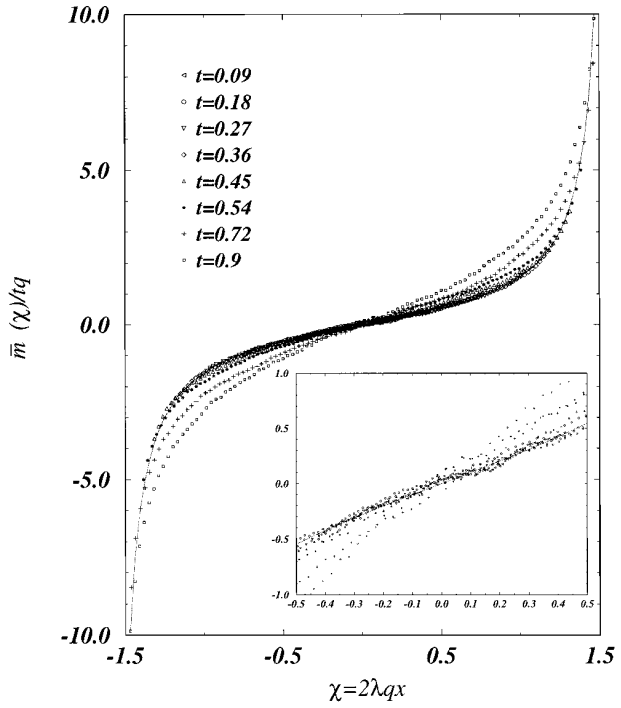

FIG. 7. Collapse plot of the average density profile, $\overline{m_j}$, to the form $m_{\mathrm{MF}}(\chi)/tq=\tan(\chi)$, with $\chi=2\lambda qx$, determined from simulation of $N=100$ chains at different t. The collapse function expected from MF theory, $\tan(\chi)$, is also plotted (solid line), and $q(\lambda)$'s are computed fitting this function (see also Fig. 5). The inset displays the central part of the profile.

We have exploited the simplifying features of the dynamics in two ways:

(A) By making a systematic expansion in the powers of the driving field t for the density and the correlation functions.

(B) By making on an appropriate level a mean field assumption for the correlation function.

Calculating a number of terms in the expansion in powers of t, we find that the solution starts to depend for large N only on the combination $\lambda=Nt^2$. For instance, the density profile of the chain [see Eq. (25)] obtains the form

$$\langle m_j\rangle=t\widetilde{m}(x;\lambda), \tag{55}$$

with x the scaled position variable [see Eq. (23)]. This observation is recovered in the mean field solution although the mean field functional form of $\widetilde{m}(x;\lambda)$ differs from the true solution. The overall shape as predicted by the mean assumption represents in a remarkable way the simulations of the model.

In fact, it is possible to take this scaling limit directly in the equations and so derive a scaled hierarchy for the density and the correlations functions (see Sec. V). By expanding in powers of λ the hierarchy is soluble (and reproduces of course the scaling limit of the more primitive expansion in powers of t). The terms in the expansion are polynomials in x, which simplifies their calculation greatly. For the determination of the coefficients of the polynomials one has to satisfy a set of linear equations that is larger than the number of coefficients to play with. However, the set turns out to have the right interdependence to allow a unique solution.

The correlations in the chain are built up from the boundaries and show an unexpected behavior. For small λ the correlations are small but significantly different from mean field predictions. In the large λ limit we see the disappearance of these effects, the density profile behavior, $\langle m_j\rangle$, at fixed t and for increasing λ displays an almost flat profile in the bulk, characteristic of a random environment, with two opposite and sharp wings at the ends. Such two localized excesses of density are sufficient to maintain the current through the whole chain. This is the reason why the MF approximation does so well in the large λ limit.

In the RDM neither an expansion in powers of t is possible nor a meaningful mean field assumption. The scaling behavior of the RDM, as it is suggested by simulations of the model, involves the combination Nt [4,7,8]. The drift velocity is much slower than the result we find here and depends in the weak field limit on the combination t/N [4,5,7,8]. Also it is not likely that the shape of the density is a function of the parameter x, which varies on the scale N. There is evidence that near the endpoints the shape varies on the scale $N^{1/2}$ [11].

Given the fact that the two types of motion are simultaneously present in the dynamics (before the map on the one-dimensional sequence is made) one wonders what the influence of the processes considered here will be in higher dimensional matrices. We think that it is minor on the basis of the following argument. One could strip the chain from its removable hairpins before the map on the 1D sequence is made. The dynamics of this backbone would quite accurately follow the rules of the RDM. The creation and destruction of the removable hairpins is fast compared to the changes in the chain due to the end point motion. Thus incorporating these processes will lead to a minor slowdown of the overall motion, which is dominated by the non-removable obstacles in the chain.

This observation is in line with the calculations of Canpolat *et al.* [12], who consider single- and double-bond jumps. The latter are similar to our removable hairpins' flipping. They argue that the double-bond jumps give a renormalization of the single-bond motion and do not change the relating physics.

In principle the phenomenon considered here could generate the sort of kink instabilities leading to what is called ''tube leakage'' [13], not comprised by repton models. However, such effects do happen in a range of fields very strong compared to the limit combination considered here. As we sit in the almost purely diffusive limit ($\varepsilon\to 0$), it becomes rather unlikely that a removable hairpin develops into such a size that it dominates the whole chain behavior.

We have actually seen how in a linear system a strong current is combined to a weak correlation between equal displacements. This observation should apply also to the linear segments of the tube in the general RDM, and unremovable hairpins should then mainly be responsible for the slow t/N drift.

ACKNOWLEDGMENTS

We thank H. J. Hilhorst for stimulating discussions. G. S. was financially supported by Stichting voor Fundamenteel Onderzoek der Materie (FOM).

APPENDIX A: SPINLIKE FORMULATION AND SYMMETRIES

As already stressed in Sec. III, operator $m_j = n_j - \frac{1}{2}$ possesses the features of a spin-$\frac{1}{2}$ variable. The analogy with spin systems can be made more explicit, because the whole algebra can be rephrased into spin language. Indeed,

$$a_j^\dagger = \begin{pmatrix} 0 & 1 \\ 0 & 0 \end{pmatrix} = \frac{1}{2}(\sigma_j^x + \imath\sigma_j^y) = \frac{1}{2}\sigma^\dagger, \tag{A1a}$$

$$a_j = \begin{pmatrix} 0 & 0 \\ 1 & 0 \end{pmatrix} = \frac{1}{2}(\sigma_j^x - \imath\sigma_j^y) = \frac{1}{2}\sigma^-, \tag{A1b}$$

$$n_j = \begin{pmatrix} 1 & 0 \\ 0 & 0 \end{pmatrix} = \frac{1}{2}(1 + \sigma_j^z), \tag{A1c}$$

$$m_j = \frac{1}{2}\begin{pmatrix} 1 & 0 \\ 0 & -1 \end{pmatrix} = \frac{1}{2}\sigma_j^z, \tag{A1d}$$

where $\sigma^{x,y,z}$ are the well known Pauli matrices, and the possible states for a segment are

$$|+1\rangle = \begin{pmatrix} 1 \\ 0 \end{pmatrix}; \quad |0\rangle = \begin{pmatrix} 0 \\ 1 \end{pmatrix}. \tag{A2}$$

In spin language $\mathcal{H}$ becomes

$$\mathcal{H} = \frac{(B+B^{-1})}{4}\left\{ \sum_{j=1}^{N-1} (\vec{\sigma}_j \cdot \vec{\sigma}_{j+1}) + 2\sigma_1^x - 2 + 2\sigma_N^x - 2 + t(\sigma_N^z - \sigma_1^z) - \imath t\left[\sum_{j=1}^{N-1} (\vec{\sigma}_j \times \vec{\sigma}_{j+1})^z + 2\sigma_1^y - 2\sigma_N^y \right] \right\}, \tag{A3}$$

where $t = (B - B^{-1}/B + B^{-1}) = \tanh\dfrac{\varepsilon}{2}$.

$\mathcal{H}$ possesses two evident symmetries, first it is invariant under the transformation

$$\begin{gathered} \sigma_j^z \to -\sigma_j^z, \\ \sigma_j^x \to \sigma_j^x, \\ \sigma_j^y \to -\sigma_j^y, \\ t \to -t, \end{gathered} \tag{A4}$$

exchanging $+1$'s with 0's under field inversion. This implies

$$\langle m_j \rangle(t) = \tfrac{1}{2}\langle \sigma_j^z \rangle(t) = -\langle \sigma_j^z \rangle(-t) = -\langle m_j \rangle(-t). \tag{A5}$$

Hence, $\langle m_j \rangle(t)$ is odd in t. Likewise, the average of any product of an odd (even) number of different m_j's is odd (even) in t.

A second transformation leaving $\mathcal{H}$ invariant is

$$\begin{gathered} \sigma_j^z \to -\sigma_j^z, \\ j \to N+1-j, \end{gathered} \tag{A6}$$

which exchanges the role of $+1$'s and 0's, and implies $\langle m_j \rangle$ is antisymmetric around the middle point of the chain, since

$$\langle m_j \rangle = -\langle m_{N+1-j} \rangle \tag{A7}$$

and then $\langle m_{(N+1/2)} \rangle = 0$.

APPENDIX B: PERTURBATIVE THEORY OF STATIONARY CORRELATION FUNCTIONS

As explained in Sec. III, the stationary equation for the average of an arbitrary number of density operators (with different indices) is derived imposing $\langle [m_j m_l \cdots, \mathcal{H}] \rangle = 0$. The commutator average is straightforwardly calculated in the spin formalism developed in the preceding section because the definition of $\langle s|$ implies

$$\begin{gathered} \langle s|\sigma_j^x \mathcal{O}(\mathbf{y})|P(\tau)\rangle = \langle \mathcal{O}(\tau) \rangle; \\ \langle s|\sigma_j^y \mathcal{O}(\mathbf{y})|P(\tau)\rangle = \imath\langle \sigma_j^z \mathcal{O}(\tau) \rangle. \end{gathered} \tag{B1}$$

So everything may ultimately be expressed in terms of average products of m_j's.

To calculate the density-density correlation, $\langle m_j m_l \rangle$, we must consider

$$0 = \langle [m_j m_l, \mathcal{H}] \rangle = \langle m_j [m_l, \mathcal{H}] + [m_j, \mathcal{H}] m_l \rangle. \tag{B2}$$

The detailed set of equations is then

$$\begin{aligned} 4\langle m_j m_l \rangle = {} & \langle m_{j-1} m_l \rangle + \langle m_{j+1} m_l \rangle + \langle m_j m_{l-1} \rangle + \langle m_j m_{l+1} \rangle \\ & + 2t[\langle m_{j-1} m_j m_l \rangle - \langle m_j m_{j+1} m_l \rangle + \langle m_j m_{l-1} m_l \rangle \\ & - \langle m_j m_l m_{l+1} \rangle] \quad (2 \leqslant j \leqslant l-2; l \leqslant N-1), \end{aligned} \tag{B3a}$$

$$\begin{aligned} 4\langle m_1 m_l \rangle = {} & -\frac{t}{2}\langle m_l \rangle - \langle m_1 m_l \rangle + \langle m_2 m_l \rangle + \langle m_1 m_{l-1} \rangle \\ & + \langle m_1 m_{l+1} \rangle + 2t[-\langle m_1 m_2 m_l \rangle + \langle m_1 m_{l-1} m_l \rangle \\ & - \langle m_1 m_l m_{l+1} \rangle] \quad (3 \leqslant l \leqslant N-1), \end{aligned} \tag{B3b}$$

$$\begin{aligned} 4\langle m_j m_N \rangle = {} & \frac{t}{2}\langle m_j \rangle - \langle m_j m_N \rangle + \langle m_{j-1} m_N \rangle + \langle m_{j+1} m_N \rangle \\ & + \langle m_j m_{N-1} \rangle + 2t[\langle m_{j-1} m_j m_N \rangle - \langle m_j m_{j+1} m_N \rangle \\ & + \langle m_j m_{N-1} m_N \rangle] \quad (2 \leqslant j \leqslant N-2), \end{aligned} \tag{B3c}$$

$$\begin{aligned} 4\langle m_1 m_N \rangle = {} & \frac{t}{2}\langle m_1 \rangle - \frac{t}{2}\langle m_N \rangle + \frac{1}{2} - 2\langle m_1 m_N \rangle + \langle m_2 m_N \rangle \\ & + \langle m_1 m_{N-1} \rangle + 2t[-\langle m_1 m_2 m_N \rangle \\ & + \langle m_1 m_{N-1} m_N \rangle], \end{aligned} \tag{B3d}$$

$$\begin{aligned} 2\langle m_j m_{j+1} \rangle = {} & \frac{t}{2}\langle m_j \rangle - \frac{t}{2}\langle m_{j+1} \rangle + \langle m_{j-1} m_{j+1} \rangle + \langle m_j m_{j+2} \rangle \\ & + 2t[\langle m_{j-1} m_j m_{j+1} \rangle - \langle m_j m_{j+1} m_{j+2} \rangle] \\ & (2 \leqslant j \leqslant N-2), \end{aligned} \tag{B3e}$$

$$2\langle m_1 m_2\rangle = \frac{t}{2}\langle m_1\rangle - t\langle m_2\rangle - \langle m_1 m_2\rangle + \langle m_1 m_3\rangle - 2t\langle m_1 m_2 m_3\rangle, \tag{B3f}$$

$$2\langle m_{N-1} m_N\rangle = t\langle m_{N-1}\rangle - \frac{t}{2}\langle m_N\rangle - \langle m_{N-1} m_N\rangle + \langle m_{N-2} m_N\rangle + 2t\langle m_{N-2} m_{N-1} m_N\rangle. \tag{B3g}$$

The set relates only to cases with $j<l$ because $\langle m_j m_l\rangle = \langle m_l m_j\rangle$. The first equation, for j and l in the bulk has the form of a discrete Poisson equation. This is a general property for any product of different m_j's, say n. Commutation with the first part of Hamiltonian (A3), the scalar product, yields a finite difference equation of the second order for the n-density correlation. The second term in $\mathcal{H}$, the vector product, is the origin of the contributions from the $(n+1)$-density correlation, multiplied by t. So the product of n factors couples to the product of $n+1$ factors but the open hierarchy can be closed and solved perturbatively as discussed in Sec. IV. Hereafter, we will explicitly work out a few steps of such perturbative theory.

The general equation for $m^{(n)}_{j,l}$ is

$$(D_j + D_l) m^{(n)}_{j,l} = -2[m^{(n-1)}_{j-1,j,l} - m^{(n-1)}_{j,j+1,l} + m^{(n-1)}_{j,l-1,l} - m^{(n-1)}_{j,l,l+1}] \quad (2\leqslant j<l-1; l\leqslant N-1). \tag{B4}$$

Where we define the second order finite difference as

$$D_j f_{\dots,j,\dots} \equiv f_{\dots,j-1,\dots} + f_{\dots,j+1,\dots} - 2 f_{\dots,j,\dots}. \tag{B5}$$

Moreover, since $m^{(2)}_{j,l}$ is defined for $j\neq l$ only, we can safely extend its set of values such to make Eqs. (B3e)–(B3g) formally equal to Eqs. (B3a)–(B3c), so extend validity of Eq. (B4) to $l=j+1$. This requires

$$m^{(n)}_{j,j} + m^{(n)}_{j+1,j+1} - 2m^{(n)}_{j,j+1} = \frac{m^{(n-1)}_j}{2} - \frac{m^{(n-1)}_{j+1}}{2} + 2[m^{(n-1)}_{j,j+1,j+1} - m^{(n-1)}_{j,j,j+1}] \quad (1\leqslant j\leqslant N-1). \tag{B6}$$

Likewise, extending $m^{(n)}_{j,l}$ to the boundaries $j=0,N+1$, Eq. (B4) holds also for $j=1$, $l=N$, by means of Eqs. (B3b)–(B3d), provided

$$m^{(n)}_{0,l} + m^{(n)}_{1,l} = -\frac{m^{(n-1)}_l}{2} - 2m^{(n-1)}_{0,1,l} \quad (3\leqslant l\leqslant N-1), \tag{B7a}$$

$$m^{(n)}_{j,N} + m^{(n)}_{j,N+1} = \frac{m^{(n-1)}_j}{2} + 2m^{(n-1)}_{j,N,N+1} \quad (2\leqslant j\leqslant N-2), \tag{B7b}$$

$$m^{(n)}_{0,N} + m^{(n)}_{1,N+1} + 2m^{(n)}_{1,N} = \frac{m^{(n-1)}_1}{2} - \frac{m^{(n-1)}_N}{2} - 2[m^{(n-1)}_{0,1,N} - m^{(n-1)}_{1,N,N+1}]. \tag{B7c}$$

Property (A6) implies

$$\langle m_j m_l\rangle = \langle m_{N+1-l} m_{N+1-j}\rangle, \tag{B8}$$

so Eqs. (B7) are not independent. Indeed Eq. (B7b) is the symmetry conjugate of Eq. (B7a), and Eq. (B7c) is the the sum of these two. Summarizing, $m^{(n)}_{j,l}$ is the solution of a discrete Poisson equation, (B4), with two independent boundary conditions (BC) (B6) and, say, (B7b).

Considering $m^{(2)}_{j,l}$, Eq. (B4) is homogeneous and the solution may be expressed in terms of the lattice version of planar harmonic functions (HF). Moreover, since the BC involve only $m^{(1)}_j$ and finite differences of $m^{(2)}_{j,l}$, we are to consider only HF of second order in j and l. Again the natural lattice variable $m^{(1)}_j = (2j-N-1)/4N$, which is antisymmetric under Eq. (A6). Since, in addition, Eq. (B8) has to be obeyed, there are only three admissible combinations of planar HF of second order in $m^{(1)}_j$, $m^{(1)}_l$. We thus solve the system with the ansatz

$$m^{(2)}_{j,l} = \alpha_1 m^{(1)}_j m^{(1)}_l + \alpha_2 (m^{(1)}_j - m^{(1)}_l) + \alpha_3. \tag{B9}$$

Just three independent linear equations in α_i's arise by substitution into the BC, and the final solution is

$$m^{(2)}_{j,l} = \frac{2N}{N-1} m^{(1)}_j m^{(1)}_l - \frac{N+1}{4(N-1)}(m^{(1)}_j - m^{(1)}_l) - \frac{N+1}{16(N-1)}. \tag{B10}$$

It is also easily realized that including higher order HF would not change the result. Indeed these components would have no counterpart on the right-hand side (RHS) of the BC. Their coefficients would then obey a homogeneous linear system, independent of $\alpha_{1,2,3}$, so they would be zero.

We can proceed further to calculate the first nonzero order of the three density average, $\langle m_j m_k m_l\rangle$, which is $m^{(3)}_{j,k,l}$. As before, the stationary equation is obtained setting equal to zero the average of the commutator $[m_j m_k m_l, \mathcal{H}]$. The general equation is

$$\begin{aligned}(D_j + D_k + D_j)\langle m_j m_k m_l\rangle &= -2t[\langle m_{j-1} m_j m_k m_l\rangle - \langle m_j m_{j+1} m_k m_l\rangle \\ &+ \langle m_j m_{k-1} m_k m_l\rangle - \langle m_j m_k m_{k+1} m_l\rangle + \langle m_j m_k m_{l-1} m_l\rangle \\ &- \langle m_j m_k m_l m_{l+1}\rangle] \quad (1<j<k-1, k<l-1<N-1).\end{aligned} \tag{B11}$$

Since $\langle m_j m_k m_l\rangle$ is defined essentially for $1\leqslant j<k<l\leqslant N$, special equations arise when one or more indices reach a boundary value, namely

$$\begin{aligned}\langle m_2 m_k m_l\rangle - 3\langle m_1 m_k m_l\rangle + (D_k + D_l)\langle m_1 m_k m_l\rangle &= 2t\Big[\langle m_1 m_2 m_k m_l\rangle \frac{1}{4}\langle m_k m_l\rangle - \langle m_j m_{k-1} m_k m_l\rangle \\ &+ \langle m_j m_k m_{k+1} m_l\rangle - \langle m_j m_k m_{l-1} m_l\rangle \\ &+ \langle m_j m_k m_l m_{l+1}\rangle\Big] \quad (2<k<l-1<N-1),\end{aligned} \tag{B12a}$$

$$D_j\langle m_j m_k m_{k+1}\rangle+\langle m_j m_{k-1} m_{k+1}\rangle+\langle m_j m_k m_{k+2}\rangle - 2\langle m_j m_k m_{k+1}\rangle = 2t\Big[\langle m_j m_{j+1} m_k m_{k+1}\rangle-\langle m_{j-1} m_j m_k m_{k+1}\rangle + \frac{\langle m_j m_{k+1}\rangle-\langle m_j m_k\rangle}{4}-\langle m_j m_{k-1} m_k m_{k+1}\rangle + \langle m_j m_k m_{k+1} m_{k+2}\rangle\Big] \quad (1<j<k-1<N-1). \tag{B12b}$$

Symmetry (A6) requires

$$\langle m_j m_k m_l\rangle=-\langle m_{N+1-l} m_{N+1-k} m_{N+1-j}\rangle \tag{B13}$$

so, like in the case of Eqs. (B7a) and (B7b), equations for $\langle m_j m_k m_N\rangle$ and $\langle m_j m_{j+1} m_l\rangle$ go over into Eqs. (B12a) and (B12b), respectively, by symmetry, and they do not provide further independent conditions. Equations at boundaries are again made formally equivalent to the general one by extending the set of values of our function to points adjacent to the boundaries and imposing consistency conditions on such extended values. Then considering the t expansion of $\langle m_j m_k m_l\rangle$, the coefficient $m^{(n)}_{j,k,l}$ is determined by the problem

$$(D_j+D_k+D_l)m^{(n)}_{j,k,l}=-2[m^{(n-1)}_{j-1,j,k,l}-m^{(n-1)}_{j,j+1,k,l}+m^{(n-1)}_{j,k-1,k,l} - m^{(n-1)}_{j,k,k+1,l}+m^{(n-1)}_{j,k,l-1,l}-m^{(n-1)}_{j,k,l,l+1}] \quad (1\leqslant<j<k<l\leqslant N), \tag{B14}$$

$$m^{(n)}_{0,k,l}+m^{(n)}_{1,k,l}=-\frac{m^{(n-1)}_{k,l}}{2}-2m^{(n-1)}_{0,1,k,l}\ (2<k<l-1<N-1), \tag{B15a}$$

$$m^{(n)}_{j,k,k}+m^{(n)}_{j,k+1,k+1}-2m^{(n)}_{j,k,k+1} = \frac{m^{(n-1)}_{j,k}-m^{(n-1)}_{j,k+1}}{2}-2[m^{(n-1)}_{j,k,k,k+1} - m^{(n-1)}_{j,k,k+1,k+1}] \quad (1<j<k-1<N-1), \tag{B15b}$$

which is a discrete Poisson problem in 3D with BC [Eqs. (B15a) and (B15b)] and the symmetry conjugate equations obtained by Eq. (B13). All other boundary equations, e.g., for $m^{(n)}_{1,k,N}$ or $m^{(n)}_{j,j+1,j+2}$, do not generate independent conditions. Indeed, originating from $\langle[m_j m_k m_l,\mathcal{H}]\rangle$, they yield linear combinations of conditions already imposed in Eqs. (B12a) and (B12b) and the symmetry conjugate of those. The system (B14) and (B15) is sufficient to determine the solution for $m^{(n)}_{j,k,l}$.

Concentrating on $m^{(3)}_{j,k,l}$, the general equation is homogeneous since $\langle m_j m_k m_l m_p\rangle$ is assumed to start out as $\mathcal{O}(t^4)$. The BC involve only $m^{(2)}_{j,k}$, which is a second order polynomial in $m^{(1)}_j$. Hence, we try to express $m^{(3)}_{j,k,l}$ in terms of lattice 3D HF up to third power in $m^{(1)}_j$ and linear in each variable. Nonlinear and higher power harmonics would not have counterpart in the inhomogeneous terms on the RHS of Eq. (B15), so their coefficients equal zero. Moreover, Eq. (B13) must be obeyed. Our guess for the solution is thus

$$m^{(3)}_{j,k,l}=\gamma_1 m^{(1)}_j m^{(1)}_k m^{(1)}_l+\gamma_2(m^{(1)}_j-m^{(1)}_l)m^{(1)}_k + \gamma_3(m^{(1)}_j+m^{(1)}_l)+\gamma_4 m^{(1)}_k. \tag{B16}$$

Equating the left- with right-hand side of Eq. (B15) produces a set of six linear equations in the coefficients, of which just four are linearly independent. The solution of such set is

$$\gamma_1=\frac{6N^2}{(N-1)(N-2)};\quad \gamma_2=-\frac{N(N+1)}{(N-1)(N-2)};\quad \gamma_3=-\frac{N+1}{16(N-1)};\quad \gamma_4=-\frac{(3N+2)(N+1)}{16(N-1)(N-2)}. \tag{B17}$$

At this stage we can go back to Eq. (B4) and solve it for $m^{(4)}_{j,l}$. This general equation has now a nonhomogeneous RHS, where $m^{(3)}_{j,k,l}$ provides a second order polynomial in $m^{(1)}_j$ and $m^{(1)}_l$. So $m^{(4)}_{j,l}$ is the sum of a special solution of the general equation (B4) of the form

$$s_{j,l}=\rho_1[(m^{(1)}_j)^3 m^{(1)}_l+m^{(1)}_j(m^{(1)}_l)^3]+\rho_2[(m^{(1)}_j)^3-(m^{(1)}_l)^3] + \rho_3[m^{(1)}_j(m^{(1)}_l)^2-(m^{(1)}_j)^2 m^{(1)}_l] + \rho_4[(m^{(1)}_j)^2+(m^{(1)}_l)^2], \tag{B18}$$

plus a harmonic part accounting for the BC [Eqs. (B6) and (B7)]

$$h_{j,l}=\rho_5 m^{(1)}_j m^{(1)}_l+\rho_6(m^{(1)}_j-m^{(1)}_l)+\rho_7. \tag{B19}$$

The ansatz $m^{(4)}_{j,l}=s_{j,l}+h_{j,l}$ yields a well determined system of linear equations in the coefficients ρ_i, and we obtain

$$\rho_1=\frac{8N^3}{(N-1)(N-2)};\quad \rho_2=-\frac{4N^2(N+1)}{3(N-1)(N-2)};\quad \rho_3=\frac{2N^2(N+1)}{(N-1)(N-2)};\quad \rho_4=-\frac{N^2(N+1)}{2(N-1)(N-2)};\quad \rho_5=\frac{-N^3+7N^2-4N}{3(N-1)(N-2)};\quad \rho_6=\frac{N^2-5N-6}{24(N-2)};\quad \rho_7=\frac{2N^2-N-3}{96(N-1)}. \tag{B20}$$

[1] P. G. de Gennes, *Scaling Concepts in Polymer Physics* (Cornell University Press, Ithaca, 1979).
[2] M. Rubinstein, Phys. Rev. Lett. **59**, 1946 (1987).
[3] T. A. J. Duke, Phys. Rev. Lett. **62**, 2877 (1989).
[4] B. Widom, J. L. Viovy, and A. D. Defontaines, J. Phys. I **1**, 1759 (1991).
[5] J. M. J. van Leeuwen, J. Phys. I **1**, 1675 (1991); J. M. J. van Leeuwen and A. Kooiman, Physica A **184**, 79 (1992).
[6] T. A. J. Duke, J. Chem. Phys. **93**, 9049 (1990); **93**, 9055 (1990).
[7] G. T. Barkema, J. F. Marko, and B. Widom, Phys. Rev. E **49**, 5303 (1994).
[8] M. Widom and I. Al-Lehyani, re-print cond-mat/9702142.
[9] C. Heller, T. A. J. Duke, and J. L. Viovy, Biophys. J. **34**, 249 (1994).
[10] G. T. Barkema and G. M. Schütz, Europhys. Lett. **35**, 139 (1996).
[11] D. P. Aalberts and J. M. J. van Leeuwen, Physica A **236**, 220 (1997).
[12] M. Canpolat, A. Erzan, and Ö. Pekcan, Phys. Rev. E **52**, 6904 (1995).
[13] J. M. Deutsch and T. L. Madden, J. Chem. Phys. **90**, 2476 (1989).